Water Resources Research

RESEARCH ARTICLE
10.1029/2019WR026127

A Classification of Streamflow Patterns Across the Coastal Gulf of Alaska

Christopher J. Sergeant[1,2], Jeffrey A. Falke[3], Rebecca A. Bellmore[4], J. Ryan Bellmore[5], and Ryan L. Crumley[6]

[1]College of Fisheries and Ocean Sciences, University of Alaska Fairbanks, Juneau, AK, USA, [2]Flathead Lake Biological Station, University of Montana, Polson, MT, USA, [3]Alaska Cooperative Fish and Wildlife Research Unit, U.S. Geological Survey, Fairbanks, AK, USA, [4]Southeast Alaska Watershed Coalition, Juneau, AK, USA, [5]Pacific Northwest Research Station, U.S. Department of Agriculture, Forest Service, Juneau, AK, USA, [6]Water Resources Graduate Program, Oregon State University, Corvallis, OR, USA

Key Points:
- Using a freshwater runoff model suited for snow and ice melt, we classified 13 flow regimes across coastal Gulf of Alaska watersheds
- In a region of rapid environmental change, fuzzy classification identified watersheds with potential transitional streamflow patterns
- Our results provide context for future studies evaluating the influence of hydrologic change on coastal Gulf of Alaska ecosystems

Supporting Information:
- Supporting Information S1
- Figure S1

Correspondence to:
C. J. Sergeant,
csergeant@alaska.edu

Citation:
Sergeant, C. J., Falke, J. A., Bellmore, R. A., Bellmore, J. R., & Crumley, R. L. (2020). A classification of streamflow patterns across the coastal Gulf of Alaska. *Water Resources Research*, *56*, e2019WR026127. https://doi.org/10.1029/2019WR026127

Received 8 AUG 2019
Accepted 20 JAN 2020
Accepted article online 23 JAN 2020

©2020. American Geophysical Union. All Rights Reserved.

Abstract Streamflow controls many freshwater and marine processes, including salinity profiles, sediment composition, fluxes of nutrients, and the timing of animal migrations. Watersheds that border the Gulf of Alaska (GOA) comprise over 400,000 km^2 of largely pristine freshwater habitats and provide ecosystem services such as reliable fisheries for local and global food production. Yet no comprehensive watershed-scale description of current temporal and spatial patterns of streamflow exists within the coastal GOA. This is an immediate need because the spatial distribution of future streamflow patterns may shift dramatically due to warming air temperature, increased rainfall, diminishing snowpack, and rapid glacial recession. Our primary goal was to describe variation in streamflow patterns across the coastal GOA using an objective set of descriptors derived from flow predictions at the downstream-most point within each watershed. We leveraged an existing hydrologic runoff model and Bayesian mixture model to classify 4,140 watersheds into 13 classes based on seven streamflow statistics. Maximum discharge timing (annual phase shift) and magnitude relative to mean discharge (amplitude) were the most influential attributes. Seventy-six percent of watersheds by number showed patterns consistent with rain or snow as dominant runoff sources, while the remaining watersheds were driven by rain-snow, glacier, or low-elevation wetland runoff. Streamflow classes exhibited clear mechanistic links to elevation, ice coverage, and other landscape features. Our classification identifies watersheds that might shift streamflow patterns in the near future and, importantly, will help guide the design of studies that evaluate how hydrologic change will influence coastal GOA ecosystems.

Plain Language Summary Streams provide society with many benefits, but they are being dramatically altered by climate change and human development. The volume of flowing water and the timing of high and low flows are important to monitor because we depend on reliable streamflow for drinking water, hydroelectric power, and healthy fish populations. Organizations that manage water supplies need extensive information on streamflow to make decisions. Yet directly measuring flow is cost-prohibitive in remote regions like the Gulf of Alaska, which drains freshwater from an area greater than 400,000 km^2, roughly the size of California. To overcome these challenges, a series of previous studies developed a tool to predict historical river flows across the entire region. In this study, we used 33 years of those predictions to categorize different types of streams based on the amount, variability, and timing of streamflow throughout the year. We identified 13 unique streamflow patterns among 4,140 coastal streams, reflecting different contributions of rain, snow, and glacial ice. This new catalog of streamflow patterns will allow scientists to assess changes in streamflow over time and their impact to humans and other organisms that depend on freshwater.

1. Introduction

Streamflow is an influential environmental variable that controls physical, chemical, and biological processes in freshwater (Poff & Ward, 1990) and marine ecosystems (Fredston-Hermann et al., 2016). At the coastal margin, where transitions from river to estuary to ocean occur over relatively short distances, patterns of streamflow—also termed flow regimes (Poff et al., 1997)—across time and space play an especially important ecological role. The timing and magnitude of freshwater runoff to nearshore marine areas drive not only physical habitat features such as water temperature (Whitney et al., 2017), salinity (Cloern et al., 2017), and

sediment composition (Wright, 1977) but also downstream fluxes of nutrients and organic matter (Hood et al., 2009; Hood & Berner, 2009; Whitney et al., 2018). Streamflow patterns are a strong driver of biological community composition (for example, fishes and macroinvertebrates; Carlisle et al., 2011) and the timing of animal migrations. At higher latitudes, streamflow pulses trigger the upstream spawning migration of anadromous fishes such as Pacific salmon (*Oncorhynchus* spp.) that transfer marine-derived nutrients to oligotrophic waters (Gende et al., 2002) and provide high-energy food sources to aquatic and terrestrial consumers (Levi et al., 2015; Willson & Halupka, 1995). But, the timing and net benefit of these subsidies to river ecosystems can vary widely based on the specific physical and chemical habitat characteristics of individual watersheds, and are often controlled by streamflow (Bellmore et al., 2014; Janetski et al., 2009). Therefore, gaining a deeper understanding of the linkages between coastal marine and freshwater ecosystems requires a basic understanding of streamflow patterns across large and heterogeneous landscapes.

The thousands of watersheds that border the Gulf of Alaska (GOA) comprise a largely pristine and diverse range of streams (O'Neel et al., 2015) that discharge 25% more freshwater than the Mississippi River from a drainage area only one seventh the size (Beamer et al., 2016; Dai et al., 2009). These streams provide critical ecosystem services such as abundant drinking water, hydroelectric power, and reliable fisheries for local and global food production (Johnson et al., 2019; Schoen et al., 2017). For example, in Southeast Alaska over 95% of electricity comes from hydropower facilities constructed in coastal watersheds (McDowell Group, 2016), and since 1985, rural residents of Southeast Alaska harvested on average over 50,000 salmon per year for noncommercial uses (ADFG, 2018). In Southcentral Alaska, the region including Prince William Sound and Cook Inlet, over 7,000 residents each year work in the seafood industry, and salmon account for 85% of the roughly $600 million in sales between seafood processors and their buyers (McDowell Group, 2015). Yet future climate projections predict that the timing and magnitude of streamflow will shift over time, complicating future water storage management for hydropower (Cherry et al., 2010) and leading to uncertain trends in the survival of freshwater life stages of Pacific salmon (Schoen et al., 2017).

The streams of coastal GOA have a number of general hydrologic patterns controlled by varying degrees of rain, snow, and glacial runoff (Edwards et al., 2013) that will persist through the end of the twenty-first century. But the geographic distribution of these flow regimes, which has not yet been comprehensively described, will likely shift due to warming air temperatures, increased rainfall, diminishing snowpack, and rapid glacial recession (Bieniek et al., 2014; Gardner et al., 2013;Littell et al., 2018 ; Shanley et al., 2015). As the average elevation of the snow-rain transition increases throughout the region, many watersheds with snow-driven runoff will shift toward rain-driven systems (Littell et al., 2018; Shanley et al., 2015). Climate-induced glacier loss also has a profound impact on watershed hydrology (Milner et al., 2017). Although the wet and snowy coastal climate patterns of the GOA may delay the response of flow regimes to changes in glacier mass balance (O'Neel et al., 2014), many watersheds will likely transition from glacier-melt to snow-melt-driven hydrology as glaciers recede and disappear. A necessary advancement for aquatic scientists working in the coastal GOA is to accurately catalog the current temporal and spatial patterns of streamflow across the region in order to deduce how this catalog may shift over time.

Continued research and monitoring to determine the distribution of streamflow patterns throughout the GOA and the potential impacts of streamflow change on freshwater ecosystems are vital, but, in a world of limited funding, the remoteness and vast scale of Alaska requires efficient prioritization of the resources necessary to complete this work. Tools such as streamflow classification not only assist in describing a region's spatial streamflow patterns but can also contribute to the research prioritization process and better equip scientists to craft landscape-scale inferences for studies with limited spatial scope (one to several watersheds). Streamflow classification is a widely applied practice with numerous analytical approaches, but its fundamental goal is to arrange streams into a logical set of categories (classes) based on flow regime characteristics describing flow magnitude, frequency, timing, duration, and rate of change (Olden et al., 2012; Poff et al., 1997). While hundreds of flow regime descriptors exist in previous streamflow literature, many are redundant or chosen subjectively (Olden & Poff, 2003). Our primary analytical goal was to describe the variation of streamflow patterns across the coastal GOA using an objective set of descriptors derived from flow predictions at the downstream-most point within each watershed.

In a region with relatively few streamgage records longer than 20 years and free of hydrologic alteration upstream (Figure 1), we leveraged an existing GOA hydrologic runoff model (GOA RM) that provides

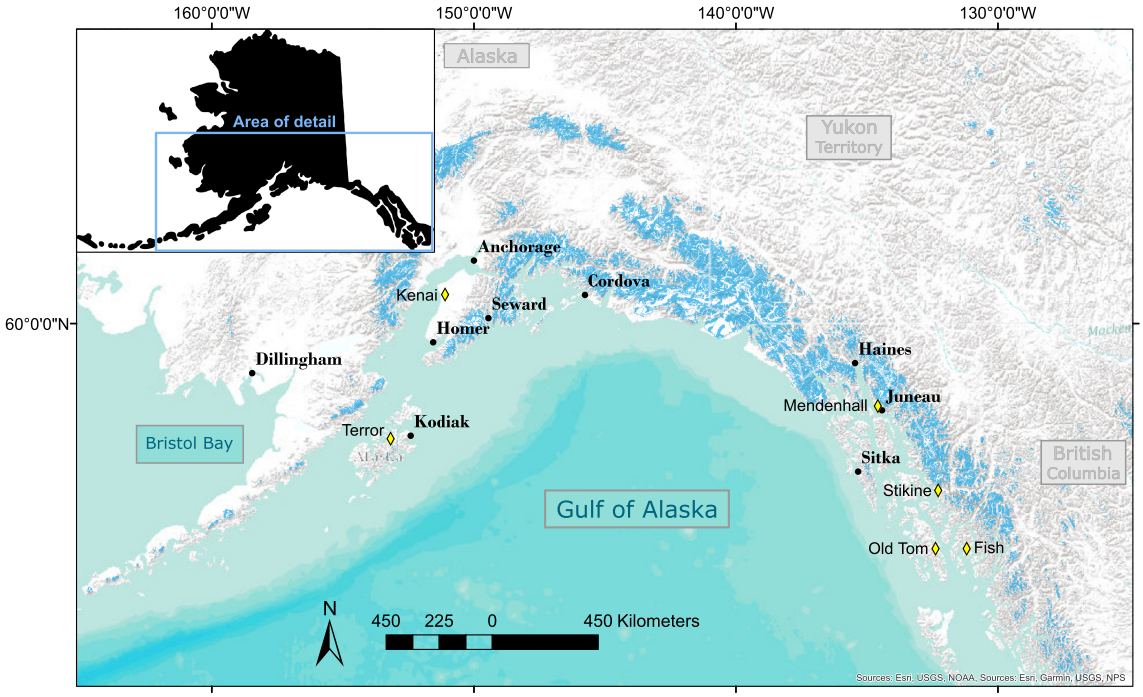


Figure 1. General overview of study area, including geographic points of interest, glacier coverage (blue shading; data from Randolph Glacier Inventory 6.0, available at https://www.glims.org/RGI/), and locations for six United States Geological Survey (USGS) streamgages (yellow diamonds) used for validating the streamflow classification (see section 3.3).

daily runoff values for a 420,300-km^2 drainage area over a 33-year historical period (Beamer et al., 2016) to classify 4,140 coastal watersheds using seven fundamental daily streamflow statistics (FDSS; Archfield et al., 2014). The resulting classes were mapped and patterns in FDSS values and land cover variables were used to assess mechanisms that drive differences in region-wide streamflow patterns. We used a Bayesian mixture model to provide inclusion probabilities for each watershed for the primary streamflow class versus secondarily assigned classes, which allowed us to identify watersheds located in transitional climate zones and with the potential to shift streamflow classes in the future (for example, from snow- to rain-driven hydrographs). Collectively, our results provide the first comprehensive description of the coastal GOA streamflow patterns by which future change can be compared.

2. Study Area

Following the geographic boundaries of Beamer et al. (2016), we defined the GOA drainage area (420,300 km^2) as starting at Dixon Entrance—the maritime area between Clarence Strait, Alaska and Hecate Strait, British Columbia (centered at approximately 54°31′N, −131°39′W)—and following the Alaskan coastline in a northwesterly direction to Wide Bay on the Alaska Peninsula (approximately 57°24′N, −156°00′W). Within the GOA drainage area are eight distinct ecological regions (Nowacki et al., 2003), moving from east to west: Alexander Archipelago, Boundary Ranges, Chugach-St. Elias Mountains, Gulf of Alaska Coast, Cook Inlet Basin, Alaska Range, Alaska Peninsula, and Kodiak Island. Common to each are extensive ice coverage, lush vegetation, steep terrain, abundant fish and wildlife, diverse stream types, and transitional climate zones reflecting a combination of wet and mild maritime influence and a drier, colder continental setting. Within this region (Figure 1), the GOA RM delineated 4,140 coastal watersheds ranging in area from 5 to 64,696 ha, including those shared between Alaska and northwestern Canada. We defined coastal watersheds as those that flow directly into the ocean. While a limited number of large rivers such as the Alsek, Copper, and Stikine penetrate the coastal mountain ranges and contribute about one third of the freshwater entering the GOA, the majority of coastal watersheds draining to the GOA are relatively small, steep, glacierized, and densely distributed along a topographically complex shoreline receiving heavy precipitation (Beamer et al., 2016; O'Neel et al., 2015). It is important to note that many of the watersheds we classified are

composed of multiple subwatersheds with hydrologic patterns that may differ from the aggregate flow patterns observed or modeled at the coastal outlet.

The GOA RM is well suited for this highly glacierized region because of its strength in predicting runoff attributable to snow and ice. Permanent snow and ice cover approximately 17% of the study area, while lakes and wetlands cover 8%. Vegetation coverage is approximately 30% forested, 27% grass/shrub, and 18% bare soil and rock (Fry et al., 2011). Elevation in the GOA drainage ranges from sea level to the highest point in North America, 6,190 m (Denali Peak, Alaska). Annual average precipitation as rain ranges over an order of magnitude from 38 cm near Anchorage to nearly 400 cm in Yakutat (McAfee et al., 2013), while annual total precipitation (including snow) averages 2.0 m water equivalent per year across the region but can be in excess of 8 m (Beamer et al., 2016).

3. Data and Methods

3.1. Modeled Streamflow and Landscape Data Acquisition

Modeled daily stream discharge values were acquired from the GOA RM from 1980 to 2012 over 1-km^2 grid cells. The GOA RM combines (1) a historical reanalysis weather product (Climate Forecast System Reanalysis; Saha et al., 2010); (2) modeled runoff for rainfall, snowmelt, and icemelt (SnowModel; Liston & Elder, 2006); (3) a soil water balance model (SoilBal; Beamer et al., 2016); and (4) a runoff routing model (HydroFlow; Liston & Mernild, 2012; Beamer et al., 2016). Model developers calibrated discharge outputs using four United States Geological Survey (USGS) streamflow gages from watersheds with long-term glacier mass balance and streamflow data (Nash-Sutcliffe efficiency = 0.89 and $r^2 = 0.93$ for modeled discharge using meteorological data from Climate Forecast System Reanalysis; Beamer et al., 2016). The four watersheds spanned combinations of rain, snow, and glacial runoff patterns for three coastal (Knik River, Mendenhall River, and Wolverine Creek) and one inland watershed (Phelan Creek). Lakewater storage, permafrost, glacial outburst floods, long-term glacier volume loss, and groundwater storage were not accounted for in the GOA RM. While these can be important considerations at the individual watershed scale, these influences were outside the scope of this study, where we focused on the geographical distribution and general diversity of streamflow patterns throughout the GOA. The GOA RM used the following data sets to derive physical watershed characteristics: (1) USGS Hydro1K North America digital elevation model (elevation and watershed delineation; https://earthexplorer.usgs.gov/); (2) 2006 National Land Cover Database (vegetation classes; Fry et al., 2011); (3) Randolph Glacier Inventory, version 3.2 (glacier ice cover; Pfeffer et al., 2014); and (4) Harmonized World Soil Data Set, version 1.2 (soil texture; Fischer et al., 2008). Complete details regarding runoff model development and model forcing data can be found in Beamer et al. (2016). To assess the mechanisms driving modeled streamflow patterns, we calculated seven land cover variables using the same data sets as the GOA RM. From the Hydro1K digital elevation model, we calculated mean and maximum elevation for each watershed. Vegetation classes from the 2006 National Land Cover Database were aggregated into proportion bare surface, forest, grass/shrub, lake/wetland, or glacierized.

3.2. Calculating Historical Streamflow Descriptors for Each Watershed

Over 200 ecologically relevant streamflow descriptors have been used by freshwater ecologists to assess river condition (for example, Richter et al., 1996), but many are redundant, and the process of determining the subset of descriptors on which to base a streamflow classification is often subjective (Archfield et al., 2014; Olden & Poff, 2003). To reduce subjectivity in selecting our streamflow descriptors, we relied on seven FDSS (Table 1) demonstrated by a recent classification of streamflow gages in the continental United States to create robust, interpretable classifications with little statistical redundancy (Archfield et al., 2014). These statistics directly measure components of the natural flow regime such as streamflow magnitude, duration and rate of change, frequency, and timing (Poff et al., 1997).

For our streamflow classification, we included only watersheds from the GOA RM with areas greater than 5 km^2 (n = 4,140; Table S1). Since digital elevation model grid cells were relatively coarse at 1 km^2, we did not have high confidence in boundary delineations for watersheds less than 5 km^2. Using the runoff model grid cell that corresponded with the coastal outlet of each watershed, we extracted daily discharge time series that spanned the modeled time period 1 October 1979 through 30 September 2012. We calculated

Table 1
Seven Fundamental Daily Streamflow Statistics (FDSS) Used to Classify Streamflow Patterns in Coastal Gulf of Alaska Watersheds

Component of natural flow regime	Streamflow descriptor	Description
Magnitude of streamflow	Mean	Mean for entire distribution of discharge values
	CV	CV for entire distribution of discharge values
	Skewness	Skewness for entire distribution of discharge values
	Kurtosis	Kurtosis for entire distribution of discharge values
Duration and rate of change	Autoregressive lag-one (AR1) correlation	AR1 correlation for entire continuous time series of discharge values
Timing	Amplitude	Magnitude of maximum discharge relative to mean
	Annual phase shift	The average day of year of maximum discharge

Note. Components of the natural flow regime are derived from Poff et al. (1997) and related to the FDSS in a manner similar to Archfield et al. (2014). Mean, coefficient of variation (CV), skewness, and kurtosis are calculated as L-moments, which are relatively unbiased compared to product moments (Hosking & Wallis, 1997).

the FDSS in Archfield et al. (2014) (Table 1) in R statistical software (version 3.4.2; R Core Team, 2017) using the "EflowStats" package (Mills & Blodgett, 2017).

3.3. Streamflow Classification

Our data matrix for classification included 4,140 rows (cases) representing individual coastal watersheds and seven columns (attributes) representing each of the FDSS calculated from the 33-year modeled streamflow time series. We classified streamflow patterns using a Bayesian mixture model implemented in AutoClass C software version 3.3.4 (NASA, Washington, DC; Cheeseman & Stutz, 1996; freely available for download at https://ti.arc.nasa.gov/tech/rse/synthesis-projects-applications/autoclass/autoclass-c/). Previous hydrologic classifications have demonstrated the utility and robustness of this unsupervised fuzzy classification method (Jones et al., 2014; Kennard et al., 2010; Reidy Liermann et al., 2012; Webb et al., 2007). In contrast with other common fuzzy clustering routines such as fuzzy k-means, AutoClass calculates classes directly from the data and does not require users to specify the number of classes. A final list of potential classifications was ranked by their marginal likelihoods. Classifications with log marginal likelihoods that differ by less than 5 are considered to be nearly equally probable (AutoClass C Documentation, 2002; https://ti.arc.nasa.gov/tech/rse/synthesis-projects-applications/autoclass/autoclass-c/). AutoClass assigned each watershed a probability of class membership to one or more classes. AutoClass also assigned relative class strength, a ratio ranging from 0 to 1 measuring the probability that attributes' distributions within a given class can predict class members (Webb et al., 2007). Within a given class of watersheds, we defined an individual watershed as having fuzzy membership when the probability of primary class membership (pm_1) was less than the global median pm_1 across all watersheds. This provided a well-defined threshold for interpreting the primary and secondary memberships across half of the watersheds within the study area.

Within AutoClass, we assigned all seven attributes to covary, creating classes that primarily represented changes in the relationships between the seven variables (Webb et al., 2007). Within AutoClass, attributes were log-transformed and modeled as normally distributed. Attributes did not require standardization because discrete distributions from each attribute were calculated directly from the data using the standard deviation from the mean. We followed previous approaches by setting the measurement error for each attribute at 10% (Jones et al., 2014; Webb et al., 2007), and set AutoClass to run 100 classification tries and stop individual tries after 500 cycles if convergence criteria were not met. All other AutoClass settings remained default.

Spatial classification patterns were visualized by color-coding watersheds according to class or pm_1 in ArcMap 10.5 (Esri, Redlands, CA). To visualize representative hydrographs for each streamflow class, we calculated the average and standard deviation of daily discharge across all years and all streams within that class. To assess whether these average hydrographs were comparable to existing long-term streamflow data, we identified six USGS streamflow gages near the Gulf of Alaska coastline with at least 27 years of data that overlapped with the GOA RM (Figure 1 and Table 2), and compared average discharge from each gage with the average discharge time series from the assigned streamflow class to further validate classification results.

Table 2
Landscape and Streamflow Classification Characteristics of USGS Streamgages (USGS, 2019) With at Least 27 Years of Observations During the Same Time Period as the GOA RM

Landscape variable	Old Tom	Terror	Fish	Mendenhall	Stikine	Kenai
Watershed area (km^2)	10	155	45	276	54,770	5,437
Latitude (DD)	55.42	57.73	55.42	58.39	56.66	60.55
Longitude (−DD)	132.38	153.18	131.19	134.58	132.28	151.10
Mean elevation (m)	132	573	233	872	1,282	547
Max elevation (m)	316	1,156	675	1,828	2,886	1,725
Proportion bare surface	0.00	0.27	0.00	0.17	0.22	0.15
Proportion forest	1.00	0.07	1.00	0.17	0.48	0.44
Proportion grass/shrub	0.00	0.59	0.00	0.12	0.20	0.26
Proportion lake/wetland	0.00	0.06	0.00	0.04	0.03	0.05
Proportion glacierized	0.00	0.00	0.00	0.49	0.07	0.10
USGS gage number	15085100	15295700	15072000	15052500	15024800	15266300
Years of record	33	27	33	31	33	33
Primary class	0	2	4	6	6	6
Pm_1	0.998	0.991	0.934	0.999	0.999	0.999
Class correlation (ρ)	0.79	0.94	0.56	0.96	0.98	0.94

Note. Landscape variables for each individual watershed were calculated directly from land cover raster data used in the GOA RM. pm_1 = probability of primary class membership; class correlation is the value of Spearman's rank correlation coefficient (ρ) for the average modeled daily discharge of a primary class versus the average empirical daily discharge from the streamgage.

4. Results

Using the seven FDSS across 4,140 coastal GOA watersheds, the most likely classification identified 13 classes of streamflow patterns. This result was overwhelmingly strong relative to alternative classifications produced by AutoClass, with a log marginal likelihood e^{12} greater than the second most likely classification. The number of individual streams belonging to each class ranged from 82 (class 12) to 601 (class 0; Table 3). Class strengths were calculated relative to class 7, which had the highest predictive strength

Table 3
Summary Statistics for the Seven Fundamental Daily Streamflow Statistics (Attributes) Used to Classify Gulf of Alaska Coastal Streamflow Patterns

	Class mean (SD)												
	Rain				Snow				Glacier		Rain-snow		LEW
Attribute	0	3	7	10	1	2	4	5	6	12	8	9	11
Mean	1.35 (2.36)	0.81 (1.44)	0.60 (0.61)	**0.33 (0.15)**	**0.41 (0.19)**	1.73 (3.75)	1.65 (3.01)	4.51 (7.40)	**51.69 (222.01)**	**20.77 (45.02)**	1.48 (4.39)	**0.28 (0.15)**	**0.33 (0.73)**
CV	0.54 (0.05)	0.55 (0.03)	0.54 (0.02)	**0.52 (0.03)**	0.60 (0.04)	**0.68 (0.04)**	0.55 (0.05)	0.52 (0.04)	0.60 (0.06)	**0.69 (0.02)**	0.55 (0.05)	0.60 (0.04)	**0.66 (0.06)**
Skewness	0.35 (0.07)	0.42 (0.05)	0.09 (0.04)	**0.31 (0.04)**	0.40 (0.07)	**0.50 (0.09)**	0.35 (0.08)	**0.27 (0.05)**	0.30 (0.07)	**0.42 (0.04)**	0.37 (0.07)	**0.47 (0.07)**	**0.71* (0.03)**
Kurtosis	0.12 (0.04)	0.15 (0.05)	0.35 (0.04)	**0.08 (0.02)**	0.10 (0.06)	0.18 (0.10)	0.10 (0.04)	**0.04 (0.02)**	**0.00 (0.04)**	**0.05 (0.04)**	0.12 (0.04)	0.18 (0.08)	**0.58* (0.05)**
AR(1)	0.92 (0.02)	0.92 (0.02)	0.89 (0.02)	0.90 (0.02)	0.92 (0.01)	0.93 (0.01)	0.93 (0.01)	0.93 (0.01)	0.91 (0.04)	0.88 (0.03)	0.93 (0.02)	0.93 (0.01)	0.97 (0.01)
Amplitude	0.43 (0.17)	0.44 (0.15)	**0.83* (0.07)**	**0.73 (0.09)**	0.64 (0.22)	**0.79 (0.19)**	0.32 (0.16)	**0.74 (0.17)**	**1.16* (0.08)**	**1.15* (0.03)**	**0.17 (0.13)**	**0.22 (0.06)**	**0.30 (0.05)**
Annual phase shift	**347* (16)**	**20 (20)**	**354* (4)**	**353* (5)**	**174 (15)**	**178 (14)**	**176 (32)**	**191 (11)**	**205* (7)**	**208* (5)**	77 (105)	**100 (32)**	**128 (11)**
n	601	364	288	183	532	533	332	302	308	82	216	229	170
Relative class strength	0.151	0.019	1.00	0.394	0.482	0.421	0.049	0.072	0.070	0.091	0.0017	0.038	0.190

Note. Classes are grouped by five metaclasses representing primary freshwater runoff source. The class mean for each attribute is listed with standard deviation (SD). Bolded values represent those attributes whose class means were greater than 1 SD from their global mean across all classes, and therefore were the most influential attributes that defined each class. Bolded values with an asterisk are greater than 3 SD from their global mean. For each class, *n* represents the number of streams assigned that class as a primary membership. LEW = low-elevation wetland.

Table 4
Summary Statistics Listed by Class for 10 Landscape Variables That Influence Gulf of Alaska Coastal Streamflow Patterns

	Class mean (SD)												
	Rain				Snow				Glacier		Rain-snow		LEW
Landscape variable	0	3	7	10	1	2	4	5	6	12	8	9	11
Watershed area (km^2)	19 (29)	19 (32)	12 (9)	7 (3)	8 (4)	34 (87)	28 (46)	52 (87)	994 (5989)	244 (616)	25 (74)	8 (4)	22 (48)
Latitude (DD)	57.91 (1.97)	57.31 (0.9)	55.70 (0.8)	55.98 (0.91)	58.18 (1.47)	59.61 (1.3)	58.00 (1.43)	57.58 (1.17)	59.31 (1.18)	60.18 (1.04)	57.86 (1.52)	57.82 (1.3)	60.92 (0.43)
Longitude (−DD)	139.32 (6.89)	145.60 (9.63)	136.59 (7.89)	135.62 (6.37)	139.42 (8.09)	143.99 (7.49)	140.59 (8.45)	135.95 (5.05)	141.79 (6.79)	144.22 (5.5)	142.27 (8.89)	144.01 (9.9)	150.83 (0.85)
Mean elevation (m)	177 (104)	144 (60)	130 (66)	140 (68)	299 (133)	414 (192)	257 (103)	353 (115)	666 (275)	1040 (356)	180 (89)	147 (82)	40 (30)
Maximum elevation (m)	433 (248)	346 (149)	311 (167)	331 (155)	658 (257)	868 (349)	626 (240)	857 (277)	1578 (817)	2040 (1021)	445 (216)	338 (185)	78 (68)
Proportion													
Bare surface	0.01 (0.04)	0.00 (0.01)	0.00 (0.00)	0.00 (0.00)	0.05 (0.12)	0.16 (0.20)	0.04 (0.12)	0.03 (0.08)	0.24 (0.15)	0.25 (0.16)	0.02 (0.08)	0.01 (0.05)	0.06 (0.17)
Forest	0.66 (0.31)	0.54 (0.42)	0.74 (0.37)	0.77 (0.27)	0.52 (0.36)	0.25 (0.25)	0.58 (0.36)	0.62 (0.27)	0.14 (0.16)	0.03 (0.08)	0.53 (0.4)	0.46 (0.42)	0.41 (0.37)
Grass/shrub	0.17 (0.24)	0.38 (0.42)	0.18 (0.35)	0.06 (0.19)	0.32 (0.31)	0.46 (0.26)	0.29 (0.31)	0.24 (0.21)	0.21 (0.15)	0.10 (0.12)	0.29 (0.35)	0.42 (0.43)	0.09 (0.18)
Lake/wetland	0.16 (0.25)	0.08 (0.12)	0.08 (0.13)	0.17 (0.19)	0.11 (0.16)	0.09 (0.14)	0.09 (0.15)	0.09 (0.14)	0.04 (0.07)	0.02 (0.03)	0.15 (0.19)	0.12 (0.20)	0.43 (0.36)
Glacierized	0.00 (0.01)	0.00 (0.00)	0.00 (0.00)	0.00 (0.00)	0.01 (0.06)	0.04 (0.09)	0.00 (0.03)	0.02 (0.08)	0.37 (0.22)	0.60 (0.24)	0.00 (0.01)	0.00 (0.00)	0.00 (0.00)

Note. Classes are grouped by five metaclasses representing primary freshwater runoff source. The class mean for each attribute is listed with standard deviation (SD). LEW = low-elevation wetland.

(Table 3). Timing of maximum discharge (annual phase shift) and the magnitude of maximum discharge relative to mean discharge (amplitude) were the most influential attributes defining 12 of 13 classes, whereas skewness and kurtosis of the distribution of discharge values primarily defined only a single class (class 11; Table 3).

The combination of FDSS values (Table 3) and landscape characteristics (Table 4) produced intuitive groupings among classes and highlighted the physical mechanisms driving the shape of the average hydrographs. Using the combination of landscape characteristics (primarily, proportion glacierized), average hydrograph shape, and the range of mean elevation values (Table 4) within each class, we aggregated the 13 classes into five metaclasses according to inferred primary freshwater runoff sources: rain (range of mean elevation 130–177 m), snow (257–414 m), glacier (666–1,040 m), rain-snow (147–180 m), and low-elevation wetland (40 m; Figure 2 and Table 4). The resulting spatial distribution of these metaclasses across the coastal GOA created distinct geographical zones of runoff sources that were consistent with the orographic influence of steep topography and the transition from wet and warmer maritime to drier and cooler continental climate (Figure 3).

Each metaclass of streamflow patterns had distinctive geographical, statistical, and land cover characteristics (Table 5 and Figures S1–S11). Three of the four classes (classes 0, 7, and 10) of rain-driven watersheds were marked by a predictable fall through early winter phase shift, with maximum flow dates of individual watersheds ranging from 7 September to 31 December (Figure 2 and Table 3). The annual phase shift of watersheds within class 3 occurred over a longer time window of winter through midspring, with maximum flow dates of individual watersheds ranging from 1 January to 2 May (Figure 2 and Table 3). All four rain-driven classes tended to be on west facing slopes in areas fully exposed to maritime climate patterns. Hydrographs of the four snow-driven classes had a distinct bimodal runoff pattern but did not follow an easily definable spatial pattern throughout the GOA. Three of the four snow-driven classes (1, 2, and 5) had average annual phase shifts occurring in early summer, with maximum flow dates of individual watersheds ranging from 13 May to 17 August (Figure 2 and Table 3). Even though the average annual phase shift of watersheds within class 4 still occurred during early summer, maximum flow dates of individual watersheds ranged over a much longer time window of 23 April to 19 October (Figure 2 and Table 3). Glacierized watersheds were the

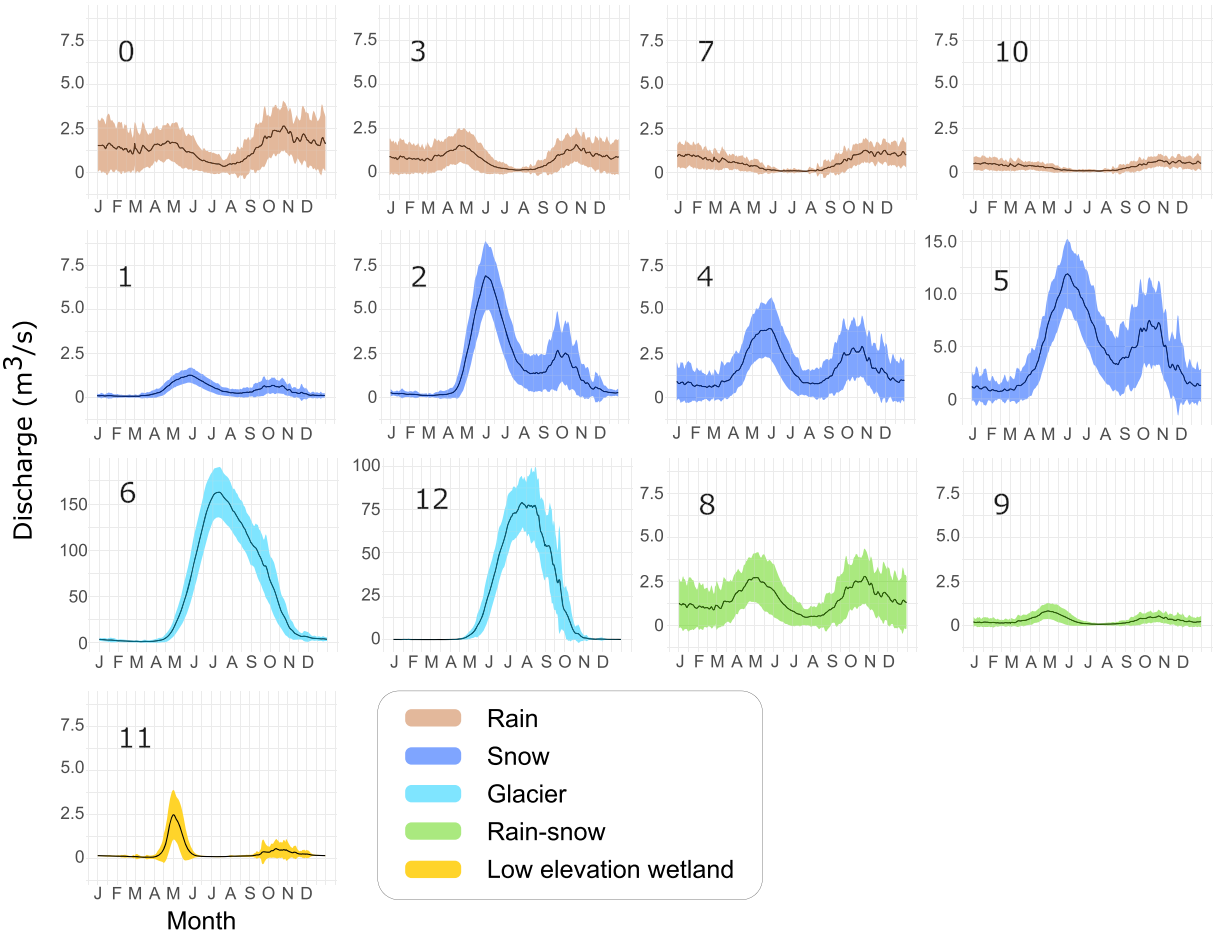


Figure 2. Representative daily discharge curves for each of 13 Gulf of Alaska coastal streamflow classes. Class numbers were assigned arbitrarily by Autoclass. The 13 classes were further grouped into five color-coded metaclasses defined by the inferred primary runoff source. Within each panel, solid lines and ribbons represent average daily discharge (m^3/s) and ±1 daily SD, respectively, calculated across every stream in that class from 33 years of modeled discharge. Note that *y* axes for classes 5, 6, and 12 vary from the remaining classes.

largest in the GOA and clearly defined by hydrographs with predictable summer annual phase shift and high amplitude (Figure 2 and Table 3). Maximum flow dates of individual glacierized watersheds (classes 6 and 12) only ranged from 2 July to 13 August. Rain-snow watersheds demonstrated dampened bimodal runoff patterns relative to snow-driven classes and tended to exhibit an average early spring annual phase shift (18 March for class 8, 10 April for class 9) with extremely unpredictable timing (Figure 2 and Table 3). For both rain-snow classes, maximum flow dates of individual watersheds could occur any day of the year. Lastly, low-elevation wetland watersheds (class 11) were found only along the shoreline of Cook Inlet and were defined by unique hydrographs relative to the other coastal GOA streamflow classes (Figure 2). Average annual phase shift occurs in May, with maximum flow dates of individual watersheds ranging from 18 March to 28 May (Figure 2 and Table 3). Low flows during the remainder of the year created distributions of daily discharge values with high skewness and kurtosis.

Across all watersheds, median primary class membership (pm_1) = 0.93. Fuzzy watersheds, which we defined as those with $pm_1 < 0.93$ ($n = 2{,}058$), tended to have intermediate hydrographs falling between the average curves of their assigned primary and secondary classes (Figure 4). Watersheds with the lowest membership probabilities were primarily grouped within the Alexander Archipelago (southeastern GOA), Prince William Sound (west of Cordova), and Kodiak Island (southwestern GOA; Figure 5). Five pairs of classes had the greatest number of fuzzy memberships (three snow-driven pairs, 1–2, 1–4, 1–5, and two rain-driven pairs 10–0, 7–10; Figure 6). Of the 2,058 fuzzy watersheds, 68% had secondary membership in the same meta-class, while 32% were secondarily assigned to different metaclasses. Of the 663 fuzzy watersheds secondarily

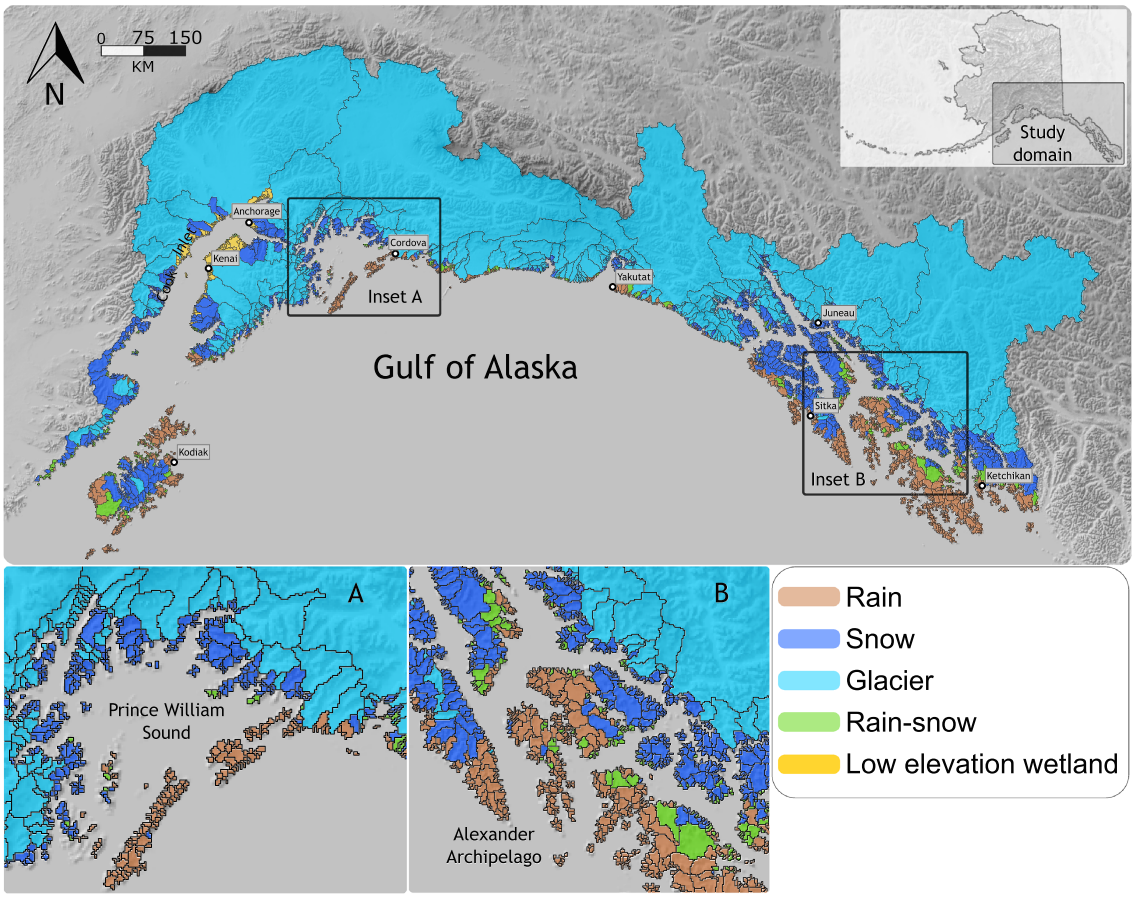


Figure 3. Spatial distribution of Gulf of Alaska coastal streamflow classes. The 13 classes were color coded by the five metaclasses defined by the inferred primary runoff source. Black lines delineate individual watersheds. Insets A and B are zoomed in to illustrate streamflow diversity in areas with abundant small watersheds.

assigned to different metaclasses, 40% were classified between rain and rain-snow, 29% between snow and glacier, 26% between snow and rain-snow, 3% between snow and rain, 2% between snow and low-elevation wetland, and 0.3% between rain-snow and low-elevation wetland (Figure 6).

We found good correspondence between the shapes of empirical hydrographs from six long-term USGS streamflow gages near the GOA coastline and modeled average hydrographs from the streamflow class to which each gaged stream was primarily assigned (Figure 7). Although mean discharge was used as the classification variable because flow magnitude is such an important control for various ecological dynamics, specific discharge is shown in Figure 7 to better distinguish differences between classes. While the magnitude of empirical discharge values did not always overlap with modeled hydrographs, the directionality of hydrograph time series was highly correlated (Spearman's ρ ranging from 0.56 to 0.98, all $p \ll 0.001$; 4 of 6 watersheds $\rho \geq 0.94$; Figure 7) and consistent with the notion that setting the FDSS as covarying in our classification emphasized the relationship between the FDSS more than the actual magnitude of each statistic (Webb et al., 2007). In other words, the shape of the hydrograph was more influential to the final classification than magnitude.

5. Discussion

In regions dominated by snow and ice runoff, the complexity of describing watershed response to rapid climate change (Barnett et al., 2005) highlights the importance of categorizing current streamflow patterns to assess future change. Using seven FDSS calculated from 33 years of modeled daily streamflow from the GOA RM, we described 13 streamflow classes across 4,140 coastal watersheds with clear mechanistic links between landscape characteristics and discharge patterns. The spatial distribution of classes was reflective

Table 5
Description of the Typical Geographical, Statistical, and Land Cover Characteristics of Each Streamflow Class in the Coastal GOA

Metaclass	Primary classifying attribute(s)	Class	Name	Range of characteristics of individual watersheds within each class
Rain	Predictable fall or winter annual phase shift (average day of year of maximum discharge)	0	Rain-I	Throughout GOA on mostly west facing slopes with high maritime influence; highest average discharge among the four rain-driven classes; average maximum discharge in mid-December with moderate variability; moderate wetland coverage; high primary membership probability
		3	Rain-II	Mostly on Kodiak Island and southern Alexander Archipelago; distinguished from other rain-driven classes by exhibiting average maximum discharge in January, but could occur as late as May
		7	Rain-III	Mostly southern GOA watersheds with high maritime influence; average maximum discharge reliably timed in middle to late December; maximum discharge moderately higher than average daily discharge; moderately low grass/shrub coverage
		10	Rain-IV	Mostly southern GOA watersheds with high maritime influence; lowest average discharge among the four rain-driven classes; average maximum discharge reliably timed in middle to late December; maximum discharge moderately higher than average daily discharge; low grass/shrub coverage; moderate wetland coverage
Snow	Predictable spring or summer annual phase shift	1	Snow-I	Throughout GOA, especially on mainland and eastern slopes of islands; lowest average discharge among the four snow-driven classes; average maximum discharge in late June but can occur late May to mid-August; average daily flow near median for all GOA streams
		2	Snow-II	Throughout GOA, mostly mainland and larger islands; like class 1, average maximum discharge in late June but can occur late May to mid-August; distinguished from class 1 by higher average discharge; maximum discharge much higher than average daily discharge; high discharge variability; positively skewed distribution of discharge values; moderately high bare ground coverage
		4	Snow-III	Throughout GOA with no obvious spatial pattern; average maximum discharge timing in late June, but within individual watersheds could occur from April through October; maximum discharge similar to average daily discharge
		5	Snow-IV	Throughout GOA but mostly larger watersheds in Alexander Archipelago; highest average discharge among the four snow-driven classes; average maximum discharge in mid-July with moderate variability; maximum discharge moderately higher than average daily discharge; low kurtosis and skewness of daily discharge distribution
Glacier	Predictable summer annual phase shift and high amplitude	6	Glacier-I	Largest watersheds in GOA; lower maritime influence; average maximum discharge reliably timed from July through mid-August; maximum discharge much higher than average daily discharge; distribution of daily discharge values is nearly normal; mean daily discharge much higher than all other classes; high mean elevation; high bare ground coverage; moderately low forest coverage; low wetland coverage; second highest glacier coverage
		12	Glacier-II	Second largest watersheds in GOA; lower maritime influence; average maximum discharge reliably timed from July through mid-August; maximum discharge much higher than average daily discharge; distribution of daily discharge values positively skewed; mean daily discharge is second behind class 6; higher mean elevation than all other classes; high bare ground coverage; low forest coverage; low wetland coverage; highest glacier coverage
Rain-snow	Unpredictable annual phase shift	8	Rain-snow-I	Throughout GOA; average discharge much higher than class 9; average maximum discharge mid-March but could occur any day of year in either the earlier or later mode; maximum discharge similar to average daily discharge; moderate wetland coverage; similar average hydrograph to class 4 but this class has much less predictable maximum discharge timing
		9	Rain-snow-II	Small watersheds throughout GOA, especially eastern side of Alexander Archipelago and Kodiak Island; average maximum discharge in mid-April but could occur any day of year in either the earlier or later mode; maximum discharge similar to average daily discharge; average daily discharge low among all GOA classes; distribution of daily discharge values positively skewed; similar average hydrograph to class 1 but this class has much less predictable maximum discharge timing

Table 5
(continued)

Metaclass	Primary classifying attribute(s)	Class	Name	Range of characteristics of individual watersheds within each class
Low-elevation wetland	High kurtosis and skewness	11	Wetland	Found exclusively in Cook Inlet; average maximum discharge in early May, but could occur as early as mid-March; distribution of daily discharge values positively skewed and tail heavy; average daily discharge low but variability high; high primary membership probability; lowest mean elevation; moderately low grass/shrub coverage; high wetland coverage

of the coastal GOA's steep topography and climatic transitions from wet maritime to drier, cooler continental patterns. Seventy-six percent of watersheds by number had streamflow patterns consistent with primarily rain or snow runoff sources (classes 0–5, 7, and 10). These water sources drove distinct differences in the contemporary timing and magnitude of maximum discharge that are likely to shift over time. The comprehensive snapshot of streamflow diversity provided by our analysis is important for a region experiencing such rapid environmental change. Based on climate change projections for the coastal GOA, which include warming air temperature and less precipitation falling as snow (Shanley et al., 2015), we expect that the future diversity of flow regimes will remain relatively static at a regional scale, but that runoff patterns will shift in space: glacierized watersheds will shift to snow-driven runoff, snow watersheds to rain-snow, and rain-snow watersheds to rain. The switch from snow to rain-snow watersheds in southern Alaska is expected to be widespread before the middle of the twenty-first century, and many low-elevation rain-snow watersheds may switch to rain-dominated by the end of the century (Littell et al., 2018).

The interaction of local topography and climate within individual watersheds is a critical component of streamflow patterns explicitly accounted for in the GOA RM. For example, total range of elevation within a watershed was shown to be a strong driver of streamflow patterns (Reidy Liermann et al., 2012) in Washington State, the southern portion of the Pacific Coastal Temperate Rainforest and the same ecoregion as our study area. Our results parallel this finding, as the five metaclasses of inferred primary runoff source exhibited discrete and mostly exclusive ranges of mean watershed elevation (Table 4). Future increases to the freezing line altitude will play a key role in reorganizing the streamflow patterns of coastal GOA within and across watersheds. In Glacier Bay—a steep and heavily glacierized fjord within the GOA drainage area and approximately 80 km west of Juneau, Alaska (Figure 3)—runoff forecasts predict that the annual proportion of snowfall contributing to total freshwater runoff across all watersheds will decrease from 58% to 24% by the year 2100 (Crumley et al., 2019). This dynamic is accurately reflected in our fuzzy analysis, where the majority of transitional watersheds in Glacier Bay share snow/glacier metaclasses (Figure 5).

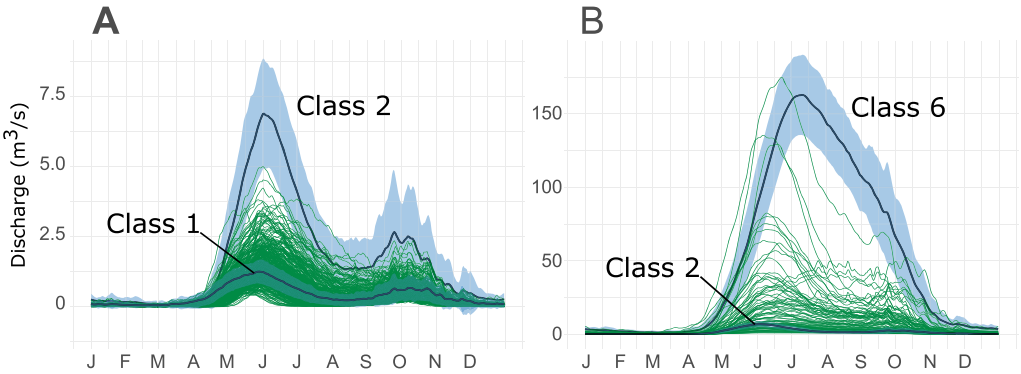


Figure 4. Modeled average annual discharge times series for individual fuzzy watersheds sharing primary and secondary membership between (a) classes 1 and 2 or (b) classes 2 and 6 (green lines). Overall modeled average annual discharge for classes 1, 2, and 6 are represented by thick lines with blue ribbons (±1 SD).

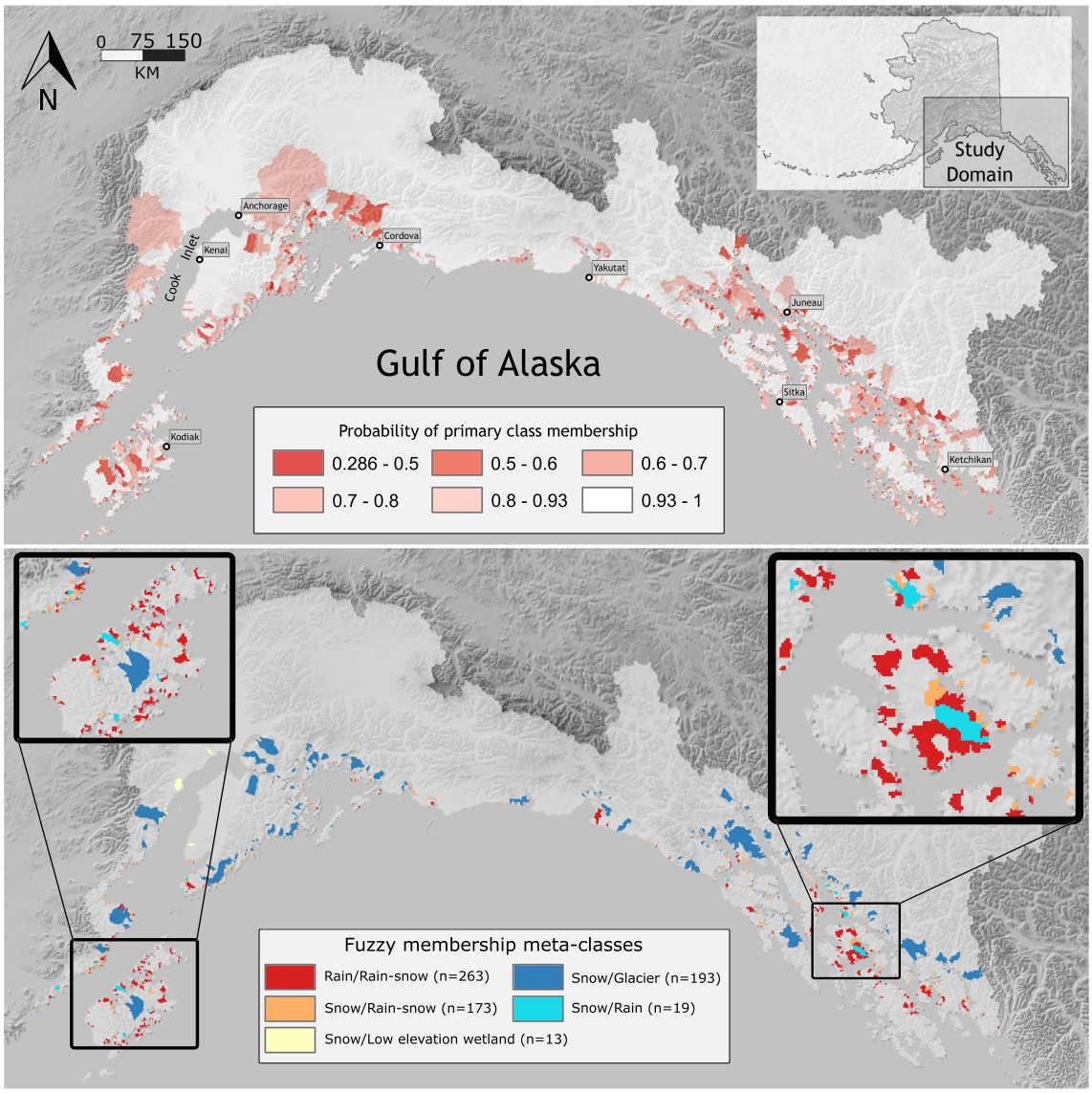


Figure 5. (top panel) Gulf of Alaska coastal watersheds color coded by primary streamflow class membership probability (pm_1). White watersheds represent those with $pm_1 > 0.93$, the median pm_1 among all watersheds. Watersheds with $pm_1 < 0.93$ are represented by red tones. (bottom panel) Fuzzy watersheds where primary and secondary classifications share two different metaclasses. Boxes represent zoomed areas for better interpretation. In both panels, watershed boundary lines have been removed to better emphasize the color patterns.

The elevation profiles of individual watersheds are also critical context with which to assess streamflow change at smaller spatial scales. For example, the Dundas River, flowing through a relatively low-elevation watershed in Glacier Bay (classified as Snow-IV; Table 5), is likely to see decreased snowfall amounts at the end of this century, as warming air temperatures are predicted to increase winter freezing line altitude approximately 300 m (Crumley et al., 2019). In contrast, winter freezing line altitude increases may be less important to the overall shape of the hydrograph in steeper and larger glacier-driven watersheds (Glacier-I and Glacier-II; Table 5), where most of the drainage area will remain within winter freezing air temperatures. As the twenty-first century progresses, the summer hydrograph of these two glacier-driven classes may steadily flatten in summer due to decreased glacial volume while the fall and winter hydrograph may increase due to greater amounts of precipitation falling as rain (Beamer et al., 2017; Crumley et al., 2019). Climate models generally agree that winter precipitation will increase throughout coastal GOA, but uncertainty exists among models regarding whether summer precipitation will increase in the region (Maloney et al., 2014).

	0	3	7	10	1	2	4	5	6	12	8	9	11
0		0.05%	0.9%	3.8%			0.1%				0.9%		
3											4.9%	1.1%	
7	3.1%			**5.5%**									
10	**5.8%**		1.1%										
1		0.05%				**6.2%**	**5.6%**	**5.7%**	0.8%			1.6%	
2					**11.0%**		0.4%	0.7%	1.9%	0.2%		0.05%	0.3%
4	0.2%	0.6%			2.0%	0.3%		2.4%			1.0%	3.0%	
5					2.1%	0.9%	3.4%		0.8%				
6					0.6%	2.2%		2.5%		2.0%			
12						0.2%			2.7%				
8	0.2%	2.2%					0.3%					0.9%	
9		3.4%			1.0%		1.4%				1.3%		0.05%
11						0.3%						0.05%	

Figure 6. A confusion matrix (after Jones et al., 2014) summarizing the percentage of secondary class memberships for coastal watersheds with a primary class membership probability less than the median probability across all streams (median $pm_1 = 0.93$; $n = 2{,}058$ watersheds with $pm_1 < 0.93$). Rows represent primary class membership, while columns represent secondary class membership. Bold, red percentages represent the classes with degree of fuzzy membership greater than 5%. Blank cells signify that no fuzzy memberships are present between the two classes.

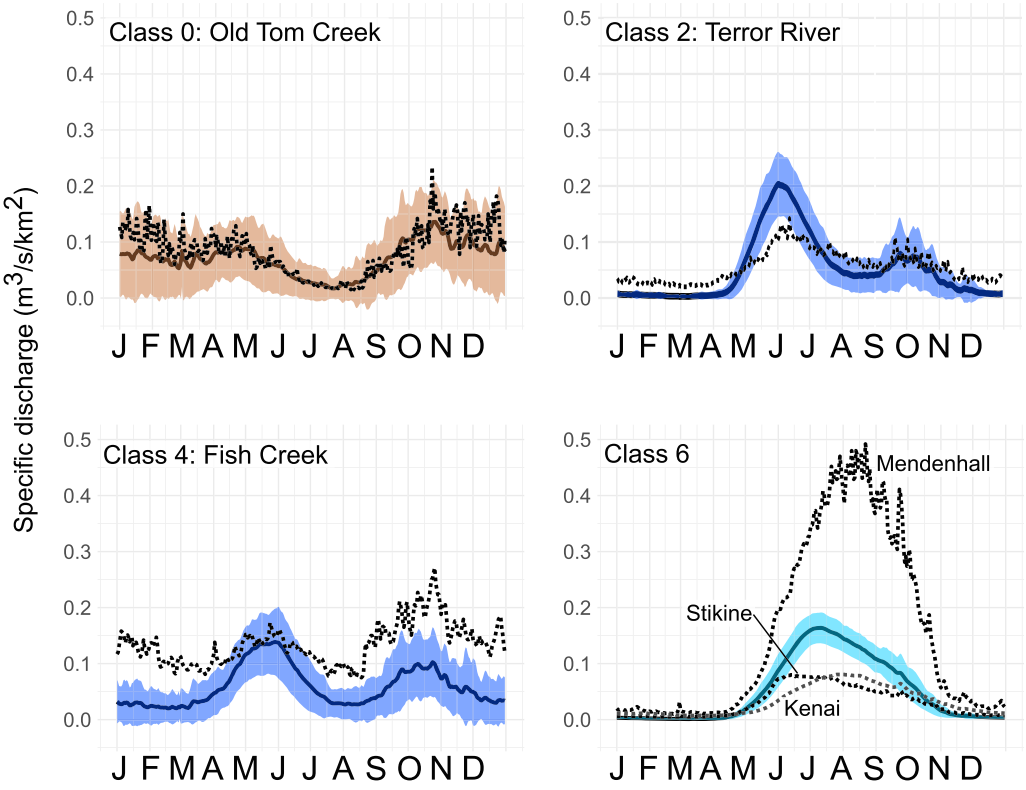


Figure 7. Comparison of modeled versus empirical daily discharge curves for Gulf of Alaska coastal streamflow classes 0, 2, 4, and 6. Within each panel, solid black lines ($m^3/s/km^2$) within colored ribbons (±1 SD) represent modeled average daily specific discharge calculated across every stream in that class from 33 years of modeled discharge. Ribbon colors match the scheme of the primary classification presented in Figure 2. Black dashed lines represent empirical average daily specific discharge measured by United States Geological Survey (USGS) streamgages assigned to the same primary class and with at least 27 years of observations during the same time period as the GOA RM.

For watersheds with snow-driven spring or early summer runoff (Snow-I, Snow-II, Snow-IV; Table 5), progressively warming air temperatures and increasing winter rain may dramatically decrease snowpack, resulting in lower magnitude spring runoff, decreased summer base flows, and shifted maximum flow timing from spring to fall (Beamer et al., 2017; Littell et al., 2018). In the Copper River watershed, the year-round snow line elevation may be increasing as quickly as 4–7 m per year (Valentin et al., 2018). Thus, many current snow-driven hydrographs may eventually resemble Rain-III, Rain-IV, Rain-snow-I, and Rain-snow-II (classes 7, 10, 8, and 9, respectively; Figure 2 and Table 5). Since the GOA RM is based primarily on historical climate data, physical runoff modeling, and soil water balance (Beamer et al., 2016), our fuzzy classification results identified watersheds located in probable zones of climatic transition that may act as sentinels of future shifts to streamflow regimes (Figure 5). For example, Kodiak Island and the central portion of southeastern Alaska between Sitka and Ketchikan have many watersheds located in transitional zones (Figure 5). Out of 4,140 watersheds, 16% ($n = 663$) had both fuzzy primary membership and a secondary membership assigned to a different runoff source (metaclass) than the primary classification (for example, a primary classification of rain-snow runoff and secondary classification of rain runoff). Nearly 95% ($n = 629$) of these same watersheds shared metaclasses that were consistent with the expected direction of future change in the GOA; the pairs included rain/rain-snow, snow/glacier, and snow/rain-snow. Although our analysis could not distinguish the current directionality of a particular watershed's hydrograph and whether it is truly shifting in the expected future direction, it is unlikely that snow watersheds will shift to glacier or rain-snow watersheds to snow.

In addition to identifying watersheds with transitional streamflow patterns, our classification results can be used to increase the scale of inference for spatially limited research conducted within one to several watersheds. For example, an observed biological phenomenon such as the temporal pattern of aquatic invertebrate productivity in a rain-driven watershed near the mouth of Prince William Sound (Inset A; Figure 3) may be widely transferable throughout the immediate area because that area is dominated by rain-driven systems. But, a study of the same dynamics in a rain-driven system on the Kenai Peninsula may have limited applicability to other watersheds in that area, which is marked mainly by glacier, snow, and low-elevation wetland streamflow patterns (see town of Kenai in Figure 3). Similarly, managers working at a subregional or local scale can use this classification to assess how proposed alterations to streamflow regimes (e.g., water diversion for hydropower) may impact streamflow diversity relative to adjacent watersheds. Water quantity is already a critical issue in coastal southern Alaska; even in a rainforest environment, extreme drought has recently caused precipitous drops in drinking water supplies and hydropower reservoir levels (KTOO, 2019a, 2019b).

In an immense and data-poor region like GOA, our streamflow classification can assist researchers to identify and strategically select study areas characterized by a range of biological or physical characteristics that could be studied across different classes of streamflow. Although we did not choose a broader set of streamflow metrics with specific relevance to a focused set of ecological questions, as is common among many hydrologic classifications, previous work in the contiguous United States demonstrated that the distribution of values from 33 ecologically relevant streamflow statistics were unique and distinguishable across classification groups derived simply from the seven FDSS used here (Archfield et al., 2014). General ecological responses to different streamflow classes could include changes in riparian recruitment, native fish production, or nonnative fish colonization success (Poff et al., 2010). More specifically, Pacific salmon are a heavily studied group of fish in the coastal GOA. Streamflow patterns directly impact freshwater life stages of salmon in multiple ways (Schoen et al., 2017), such as altering migration timing (Kovach et al., 2015), increasing egg scour during winter floods (Shanley & Albert, 2014; Sloat et al., 2017), creating low dissolved oxygen events during summer low flows (Sergeant et al., 2017; see also Fellman et al., 2018; Tillotson & Quinn, 2017), or altering migratory connectivity between estuary and river mouth (Flitcroft et al., 2018; Koski, 2009). For example, researchers interested in the impacts of summer low flow to salmon migration may choose to stratify their watershed sampling frame for classes 7, 9, 10, and 11, which, relative to other classes, exhibit lower baseflow with lower variability during warmer months (Figure 2 and Table 5).

While coastal streamflow patterns can be used to assess the types of ecological questions posed above, it is important to note that some questions will require a better understanding of habitat diversity throughout the entire stream network (for example, see Moore et al., 2015), which was not assessed here. Individual watersheds in the GOA region frequently contain a mosaic of glacial, snow, and rain-fed tributaries. In

the Copper River watershed, for example, the colder and drier interior portions of the upper watershed are primarily glacial-fed, whereas tributaries closer to the river mouth are primarily rain- and snow-fed and generate 80% of total watershed runoff (Valentin et al., 2018). Some larger watersheds may offer greater overall streamflow heterogeneity and, depending on the physical or biological dynamic of interest, buffer the impacts resulting from the loss of streamflow diversity at the coastal margin. While lake storage was also not accounted for in the GOA RM, depending on total lake coverage and position of individual lakes within the stream network, we would generally expect lakes to dampen streamflow variability and delay maximum flows relative to watersheds with similar climate and geomorphology, but with less or no lake coverage (for example, see Jones et al., 2014).

6. Conclusions

This analysis provides the first comprehensive description of streamflow patterns throughout the coastal GOA, a 420,300-km^2 highly glacierized drainage area with 25% more total discharge and 9.5 times higher discharge per unit area than the Mississippi River watershed (Beamer et al., 2016; Dai et al., 2009). Across the globe, shifting flow regimes and extreme events create societal and ecological impacts that include reduced water supply for urban centers (McDonald et al., 2011), reduced suitable habitat area for endemic fish species (Ficke et al., 2007), and increased land inundation due to greater flood frequency and magnitude in some areas (Mirza et al., 2003). Our ultimate hope is that we have created an intuitive and accessible streamflow classification to guide aquatic research and monitoring throughout GOA coastal ecosystems. We envision three immediate applications of this work: (1) planning monitoring programs in watersheds that we identified as potentially transitional (for example, snow to rain), (2) increasing the scale of inference for spatially limited research, and (3) assisting researchers in selecting study areas with a range of biological or physical characteristics influenced by streamflow. Although there remains some uncertainty in how future climate shifts will affect GOA ecosystems, there is no doubt that the spatial distribution of flow regimes will shift over time, and freshwater runoff will remain a critical topic in this region, as it directly impacts water diversion activities such as hydropower production and mining, drinking water supply, and globally important fisheries.

Acknowledgments

We thank two anonymous reviewers and J. Curran for their thoughtful peer review. D. Hill and J. Beamer provided support with the Gulf of Alaska runoff model. F. Biles and D. Verbyla offered valuable advice on ArcMap workflows. We thank A. Beaudreau, F. Mueter, E. Peterson, and P. Westley for the preliminary discussions and reviews. F. Mueter also assisted with statistical coding for calculating the fundamental daily streamflow statistics. Alaska Sea Grant (project R/31-25) supported this work. J. R. Bellmore was supported by the U.S. Department of Interior Alaska Climate Adaptation Science Center. Any use of trade, firm, or product names is for descriptive purposes only and does not imply endorsement by the U.S. Government. The following data will be available as a single .zip file stored on ScienceBase at https://doi.org/10.5066/P9BHITX2):

- Autoclass input and output files
- Classification data for individual watersheds, including FDSS, land cover variables, and class membership (.csv file)
- Esri map package (.mpk file) that will allow users to recreate Figures 3 and 5 using ArcGIS and extract basic watershed-scale data such as

References

ADFG (2018). 2018 Alaska commercial salmon harvests—Exvessel values (preliminary data). Retrieved from https://www.adfg.alaska.gov/static/fishing/pdfs/commercial/2018_preliminary_salmon_summary_table.pdf

Archfield, S. A., Kennen, J. G., Carlisle, D. M., & Wolock, D. M. (2014). An objective and parsimonious approach for classifying natural flow regimes at a continental scale. *River Research and Applications*, *30*(9), 1166–1183. https://doi.org/10.1002/rra

Barnett, T. P., Adam, J. C., & Lettenmaier, D. P. (2005). Potential impacts of a warming climate on water availability in snow-dominated regions. *Nature*, *438*(7066), 303–309. https://doi.org/10.1038/nature04141

Beamer, J. P., Hill, D. F., Arendt, A., & Liston, G. E. (2016). High-resolution modeling of coastal freshwater discharge and glacier mass balance in the Gulf of Alaska watershed. *Water Resources Research*, *52*, 3888–3909. https://doi.org/10.1002/2015WR018457

Beamer, J. P., Hill, D. F., McGrath, D., Arendt, A., & Kienholz, C. (2017). Hydrologic impacts of changes in climate and glacier extent in the Gulf of Alaska watershed. *Water Resources Research*, *53*, 7502–7520. https://doi.org/10.1002/2016WR020033

Bellmore, J. R., Fremier, A. K., Mejia, F., & Newsom, M. (2014). The response of stream periphyton to Pacific salmon: Using a model to understand the role of environmental context. *Freshwater Biology*, *59*(7), 1437–1451. https://doi.org/10.1111/fwb.12356

Bieniek, P. A., Walsh, J. E., Thoman, R. L., & Bhatt, U. S. (2014). Using climate divisions to analyze variations and trends in Alaska temperature and precipitation. *Journal of Climate*, *27*(8), 2800–2818. https://doi.org/10.1175/JCLI-D-13-00342.1

Carlisle, D. M., Wolock, D. M., & Meador, M. R. (2011). Alteration of streamflow magnitudes and potential ecological consequences: a multiregional assessment. *Frontiers in Ecology and the Environment*, *9*(5), 264–270. https://doi.org/10.1890/100053

Cheeseman, P., & Stutz, J. (1996). Bayesian classification (Autoclass): theory and results. In U. Fayyad, et al. (Eds.), *Advances in knowledge discovery and data mining* (pp. 153–180). Cambridge, MA: AAAI Press and MIT Press.

Cherry, J. E., Walker, S., Fresco, N., Trainor, S., & A. Tidwell. (2010). Impacts of climate change and variability on hydropower in Southeast Alaska: Planning for a robust energy future. Retrieved from https://alaskafisheries.noaa.gov/sites/default/files/ccv_hydro_se.pdf

Cloern, J. E., Jassby, A. D., Schraga, T. S., Nejad, E., & Martin, C. (2017). Ecosystem variability along the estuarine salinity gradient: Examples from long-term study of San Francisco Bay. *Limnology and Oceanography*, *62*(S1), S272–S291. https://doi.org/10.1002/lno.10537

Crumley, R. L., Hill, D. F., Beamer, J. P., & Holzenthal, E. (2019). Hydrologic diversity in Glacier Bay Alaska: Spatial patterns and temporal change. *The Cryosphere*, *13*, 1597–1619. https://doi.org/10.5194/tc-13-1597-2019

Dai, A., Qian, T., Trenberth, K. E., & Milliman, J. D. (2009). Changes in continental freshwater discharge from 1948 to 2004. *Journal of Climate*, *22*(10), 2773–2792. https://doi.org/10.1175/2008JCLI2592.1

Edwards, R. T., D'Amore, D. V., Norberg, E., & Biles, F. (2013). Riparian ecology, climate change, and management in North Pacific Coastal Rainforests. In G. Orians & J. Schoen (Eds.), *North Pacific temperate rainforests: ecology and conservation* (pp. 43–72). Seattle, WA: University of Washington Press.

Fellman, J. B., Hood, E., Nagorski, S., Hudson, J., & Pyare, S. (2018). Interactive physical and biotic factors control dissolved oxygen in salmon spawning streams in coastal Alaska. *Aquatic Sciences*, *81*(1), 1–11. https://doi.org/10.1007/s00027-018-0597-9

watershed ID, drainage area, primary class assignment, and primary class membership probability (for users interested in extracting more information such as secondary class membership and land cover data, Watershed ID in this file can be cross-referenced with Watershed ID in the .csv file above)
- R Shiny application to create Figure 3 map and extract classification and land cover variables for individual watersheds (also viewable at https://southeastakwatershedcoalition.shinyapps.io/watershed_classification/).

Ficke, A. D., Myrick, C. A., & Hansen, L. J. (2007). Potential impacts of global climate change on freshwater fisheries. *Reviews in Fish Biology and Fisheries*, *17*(4), 581–613.

Fischer, G., Nachtergaele, F. O., Pryler, S., van Velthuizen, H., Verelst, L., & Wiberg, D. (2008). Global Agro-ecological Zones Assessment for Agriculture (GAEZ 2008), International Institute for Applied Systems Analysis, Laxenburg, Austria.

Flitcroft, R. L., Arismendi, I., & Santelmann, M. V. (2018). A review of habitat connectivity research for Pacific salmon in marine, estuary, and freshwater environments. *Journal of the American Water Resources Association*, *55*(2), 1–12. https://doi.org/10.1111/1752-1688.12708

Fredston-Hermann, A., Brown, C. J., Albert, S., Klein, C. J., Mangubhai, S., Nelson, J. L., et al. (2016). Where does river runoff matter for coastal marine conservation? *Frontiers in Marine Science*, *3*, 1–10. https://doi.org/10.3389/fmars.2016.00273

Fry, J. A., Xian, G., Jin, S. M., Dewitz, J. A., Homer, C. G., Yang, L. M., et al. (2011). Completion of the 2006 national land cover database for the conterminous United States. *Photogrammetric Engineering & Remote Sensing*, *77*(9), 858–864.

Gardner, A. S., Moholdt, G., Cogley, J. G., Wouters, B., Arendt, A. A., Wahr, J., et al. (2013). A reconciled estimate of glacier contributions to sea level rise: 2003 to 2009. *Science*, *340*(6134), 852–857. https://doi.org/10.1126/science.1234532

Gende, S. M., Edwards, R. T., Willson, M. F., & Wipfli, M. S. (2002). Pacific salmon in aquatic and terrestrial ecosystems. *Bioscience*, *52*(10), 917–928. https://doi.org/10.1641/0006-3568(2002)052[0917:PSIAAT]2.0.CO;2

Hood, E., & Berner, L. (2009). Effects of changing glacial coverage on the physical and biogeochemical properties of coastal streams in southeastern Alaska. *Journal of Geophysical Research*, *114*, G03001. https://doi.org/10.1029/2009JG000971

Hood, E., Fellman, J., Spencer, R. G., Hernes, P. J., Edwards, R., D'Amore, D., & Scott, D. (2009). Glaciers as a source of ancient and labile organic matter to the marine environment. *Nature*, *462*(7276), 1044–1047. https://doi.org/10.1038/nature08580

Hosking, J. R. M., & Wallis, J. R. (1997). *Regional frequency analysis: An approach based on L-moments*. UK: Cambridge University Press. https://doi.org/10.1017/cbo9780511529443

Janetski, D. J., Chaloner, D. T., Tiegs, S. D., & Lamberti, G. A. (2009). Pacific salmon effects on stream ecosystems: A quantitative synthesis. *Oecologia*, *159*(3), 583–595. https://doi.org/10.1007/s00442-008-1249-x

Johnson, A. C., Bellmore, J. R., Haught, S., & Medel, R. (2019). Quantifying the monetary value of Alaska national forests to commercial Pacific salmon fisheries. *North American Journal of Fisheries Management*, *39*(6), 1119–1131. https://doi.org/10.1002/nafm.10364

Jones, N. E., Schmidt, B. J., Melles, S. J., & Brickman, D. (2014). Characteristics and distribution of natural flow regimes in Canada: A habitat template approach. *Canadian Journal of Fisheries and Aquatic Sciences*, *71*(11), 1616–1624. https://doi.org/10.1139/cjfas-2014-0040

Kennard, M. J., Pusey, B. J., Olden, J. D., MacKay, S. J., Stein, J. L., & Marsh, N. (2010). Classification of natural flow regimes in Australia to support environmental flow management. *Freshwater Biology*, *55*(1), 171–193. https://doi.org/10.1111/j.1365-2427.2009.02307.x

Koski, K. V. (2009). The fate of coho salmon nomads: The story of an estuarine-rearing strategy promoting resilience. *Ecology and Society*, *14*(1).

Kovach, R. P., Ellison, S. C., Pyare, S., & Tallmon, D. A. (2015). Temporal patterns in adult salmon migration timing across southeast Alaska. *Global Change Biology*, *21*(5), 1821–1833. https://doi.org/10.1111/gcb.12829

KTOO. (2019a). Alaska communities used to have plenty of fresh water. Then came severe drought. Retrieved from https://www.ktoo.org/2019/09/09/alaska-communities-used-to-have-plenty-of-fresh-water-then-came-severe-drought/

KTOO. (2019b). Ongoing drought conditions mean Ketchikan could be renting backup generators through the fall. Retrieved from https://www.ktoo.org/2019/06/19/ongoing-drought-conditions-mean-ketchikan-could-be-renting-backup-generators-through-the-fall/

Levi, T., Wheat, R. E., Allen, J. M., & Wilmers, C. C. (2015). Differential use of salmon by vertebrate consumers: Implications for conservation. *PeerJ*, *3*, e1157. https://doi.org/10.7717/peerj.1157

Liston, G. E., & Elder, K. (2006). A distributed snow-evolution modeling system (SnowModel). *Journal of Hydrometeorology*, *7*, 1259–1276. https://doi.org/10.1175/JHM548.1

Liston, G. E., & Mernild, S. H. (2012). Greenland freshwater runoff. Part I: A runoff routing model for glaciated and nonglaciated landscapes (HydroFlow). *Journal of Climate*, *25*(17), 5997–6014. https://doi.org/10.1175/JCLI-D-11-00591.1

Littell, J., McAfee, S., & Hayward, G. (2018). Alaska snowpack response to climate change: Statewide snowfall equivalent and snowpack water scenarios. *Water*, *10*(5), 668. https://doi.org/10.3390/w10050668

Maloney, E. D., Camargo, S. J., Chang, E., Colle, B., Fu, R., Geil, K. L., et al. (2014). North American climate in CMIP5 experiments: Part III—Assessment of twenty-first-century projections. *Journal of Climate*, *27*(6), 2230–2270. https://doi.org/10.1175/JCLI-D-13-00273.1

McAfee, S. A., Guentchev, G., & Eischeid, J. K. (2013). Reconciling precipitation trends in Alaska: 1. Station-based analyses. *Journal of Geophysical Research: Atmospheres*, *118*, 7523–7541. https://doi.org/10.1002/jgrd.50572

McDonald, R. I., Green, P., Balk, D., Fekete, B. M., Revenga, C., Todd, M., & Montgomery, M. (2011). Urban growth, climate change, and freshwater availability. *Proceedings of the National Academy of Sciences*, *108*(15), 6312–6317.

McDowell Group. (2015). The economic impact of the seafood industry in south central Alaska. (Technical Report, pp. 1-101). Juneau and Anchorage, AK. Retrieved from http://www.mcdowellgroup.net/publications/

McDowell Group. (2016). Southeast Alaska energy update and profile. (Technical Report, pp. 1-114). Juneau and Anchorage, AK. Retrieved from http://www.mcdowellgroup.net/publications/

Mills, J., & Blodgett, D. (2017). EflowStats: Hydrologic Indicator and Alteration Stats. R package version 5.0.0.

Milner, A. M., Khamis, K., Battin, T. J., Brittain, J. E., Barrand, N. E., Füreder, L., et al. (2017). Glacier shrinkage driving global changes in downstream systems. *Proceedings of the National Academy of Sciences*, *114*(37), 9770–9778. https://doi.org/10.1073/pnas.1619807114

Mirza, M. M. Q., Warrick, R. A., & Ericksen, N. J. (2003). The implications of climate change on floods of the Ganges, Brahmaputra and Meghna rivers in Bangladesh. *Climatic Change*, *57*(3), 287–318.

Moore, J. W., Beakes, M. P., Nesbitt, H. K., Yeakel, J. D., Patterson, D. A., Thompson, L. A., et al. (2015). Emergent stability in a large, free-flowing watershed. *Ecology*, *96*(2), 340–347. https://doi.org/10.1890/14-0326.1

Nowacki, G. J., Spencer, P., Fleming, M., Brock, T., & Jorgenson, T. (2003). Unified ecoregions of Alaska: 2001 (No. 2002-297). Geological Survey (US).

Olden, J. D., Kennard, M. J., & Pusey, B. J. (2012). A framework for hydrologic classification with a review of methodologies and applications in ecohydrology. *Ecohydrology*, *5*(4), 503–518. https://doi.org/10.1002/eco.251

Olden, J. D., & Poff, N. L. (2003). Redundancy and the choice of hydrologic indices for characterizing streamflow regimes. *River Research and Applications*, *19*(2), 101–121. https://doi.org/10.1002/rra.700

O'Neel, S., Hood, E., Arendt, A., & Sass, L. (2014). Assessing streamflow sensitivity to variations in glacier mass balance. *Climatic Change*, *123*(2), 329–341. https://doi.org/10.1007/s10584-013-1042-7

O'Neel, S., Hood, E., Bidlack, A. L., Fleming, S. W., Arimitsu, M. L., Arendt, A., et al. (2015). Icefield-to-ocean linkages across the northern pacific coastal temperate rainforest ecosystem. *Bioscience*, *65*(5), 499–512. https://doi.org/10.1093/biosci/biv027

Pfeffer, W. T., Arendt, A. A., Bliss, A., Bolch, T., Cogley, J. G., Gardner, A. S., et al., & The Randolph Consortium (2014). The Randolph Glacier Inventory: A globally complete inventory of glaciers. *Journal of Glaciology*, *60*(221), 537–552. https://doi.org/10.3189/2014JoG13J176

Poff, N. L., Allan, J. D., Bain, M. B., Karr, J. R., Prestegaard, K. L., Richter, B. D., et al. (1997). The natural flow regime. *Bioscience*, *47*(11), 769–784. https://doi.org/10.2307/1313099

Poff, N. L., Richter, B. D., Arthington, A. H., Bunn, S. E., Naiman, R. J., Kendy, E., et al. (2010). The ecological limits of hydrologic alteration (ELOHA): A new framework for developing regional environmental flow standards. *Freshwater Biology*, *55*(1), 147–170. https://doi.org/10.1111/j.1365-2427.2009.02204.x

Poff, N. L., & Ward, J. V. (1990). Physical habitat template of lotic systems: Recovery in the context of historical pattern of spatiotemporal heterogeneity. *Environmental Management*, *14*(5), 629–645.

R Core Team (2017). R: A language and environment for statistical computing. R Foundation for Statistical Computing, Vienna, Austria. Retrieved from https://www.R-project.org/

Reidy Liermann, C. A., Olden, J. D., Beechie, T. J., Kennard, M. J., Skidmore, P. B., Konrad, C. P., & Imaki, H. (2012). Hydrogeomorphic classification of Washington State rivers to support emerging environmental flow management strategies. *River Research and Applications*, *28*(9), 1340–1358. https://doi.org/10.1002/rra.1541

Richter, B. D., Baumgartner, J. V., Powell, J., & Braun, D. P. (1996). A method for assessing hydrologic alteration within ecosystems. *Conservation Biology*, *10*(4), 1163–1174. https://doi.org/10.1046/j.1523-1739.1996.10041163.x

Saha, S., Moorthi, S., Pan, H. L., Wu, X., Wang, J., Nadiga, S., et al. (2010). The NCEP Climate Forecast System Reanalysis. *Bulletin of the American Meteorological Society*, *91*(8), 1015–1058. https://doi.org/10.1175/2010BAMS3001.1

Schoen, E. R., Wipfli, M. S., Trammell, E. J., Rinella, D. J., Floyd, A. L., Grunblatt, J., et al. (2017). Future of Pacific salmon in the face of environmental change: Lessons from one of the world's remaining productive salmon regions. *Fisheries*, *42*(10), 538–553. https://doi.org/10.1080/03632415.2017.1374251

Sergeant, C. J., Bellmore, J. R., McConnell, C., & Moore, J. W. (2017). High salmon density and low discharge create periodic hypoxia in coastal rivers. *Ecosphere*, *8*(6), e01846. https://doi.org/10.1002/ecs2.1846

Shanley, C. S., & Albert, D. M. (2014). Climate change sensitivity index for Pacific salmon habitat in southeast Alaska. *PLoS ONE*, *9*(8), e104799. https://doi.org/10.1371/journal.pone.0104799

Shanley, C. S., Pyare, S., Goldstein, M. I., Alaback, P. B., Albert, D. M., Beier, C. M., et al. (2015). Climate change implications in the northern coastal temperate rainforest of North America. *Climatic Change*, *130*(2), 155–170. https://doi.org/10.1007/s10584-015-1355-9

Sloat, M. R., Reeves, G. H., & Christiansen, K. R. (2017). Stream network geomorphology mediates predicted vulnerability of anadromous fish habitat to hydrologic change in southeast Alaska. *Global Change Biology*, *23*(2), 604–620. https://doi.org/10.1111/gcb.13466

Tillotson, M. D., & Quinn, T. P. (2017). Climate and conspecific density trigger pre-spawning mortality in sockeye salmon (*Oncorhynchus nerka*). *Fisheries Research*, *188*, 138–148. https://doi.org/10.1016/j.fishres.2016.12.013

USGS (2019). USGS waterdata for the Nation: U.S. Geological Survey National Water Information System database, accessed 30 January 2020. Available at https://doi.org/10.5066/F7P55KJN

Valentin, M. M., Hogue, T. S., & Hay, L. E. (2018). Hydrologic regime changes in a high-latitude glacierized watershed under future climate conditions. *Watermark*, *10*(2), 128. https://doi.org/10.3390/w10020128

Webb, J. A., Bond, N. R., Wealands, S. R., Mac Nally, R., Quinn, G. P., Vesk, P. A., & Grace, M. R. (2007). Bayesian clustering with AutoClass explicitly recognises uncertainties in landscape classification. *Ecography*, *30*(4), 526–536. https://doi.org/10.1111/j.2007.0906-7590.05002.x

Whitney, E. J., Beaudreau, A. H., & Duncan, D. H. (2017). Spatial and temporal variation in the diets of Pacific *Staghorn sculpins* related to hydrological factors in a glacially influenced estuary. *Transactions of the American Fisheries Society*, *146*(6), 1156–1167. https://doi.org/10.1080/00028487.2017.1341852

Whitney, E. J., Beaudreau, A. H., & Howe, E. R. (2018). Using stable isotopes to assess the contribution of terrestrial and riverine organic matter to diets of nearshore marine consumers in a glacially influenced estuary. *Estuaries and Coasts*, *41*(1), 193–205. https://doi.org/10.1007/s12237-017-0260-z

Willson, M. F., & Halupka, K. C. (1995). Anadromous fish as keystone species in vertebrate communities. *Conservation Biology*, *9*(3), 489–497. https://doi.org/10.1046/j.1523-1739.1995.09030489.x

Wright, L. D. (1977). Sediment transport and deposition at river mouths: A synthesis. *Geological Society of America Bulletin*, *88*(6), 857–868. https://doi.org/10.1130/0016-7606(1977)88<857:STADAR>2.0.CO;2